Short Communication

Corrosion behavior of incoloy825 alloy in 3.5% NaCl solution containing different concentrations of NaHSO₃

Min Zhu[*]*, Jinlin Yang, Yuanbin Chen, Jian Zhou, Yongfeng Yuan, Shaoyi Guo*

School of Mechanical Engineering & Automation, Zhejiang Sci-Tech University, Hangzhou 310018, PR China
[*]E-mail: zmii666@126.com

The corrosion behavior of incoloy825 alloy in 3.5% NaCl solution containing different concentrations of NaHSO₃ was studied using electrochemical measurements, wet/dry cycle corrosion test and surface analysis technology. The results show that the corrosion potential shifts negatively, and then moves positively with the increase of NaHSO₃ concentration. Meanwhile, the film resistance R_f and charge transfer resistance R_{ct} both decline firstly and then rise as the concentration change. And the anode polarization curves display different characteristics of passivation or activation. As the increasing concentration of NaHSO₃, the corrosion rate of alloy increases firstly and then decreases. In the solution, the corrosion form of the alloy is mainly pitting corrosion, and the addition of NaHSO₃ increases the degree of pitting. The variation of the corrosion resistance as the increase of NaHSO₃ concentration may be attributed to the combined actions of solution acidification and competitive adsorption.

1. INTRODUCTION

Incoloy825 nickel-based alloy has been widely used in many industries, for example, ocean engineering, chemical engineering and aviation field, which is attributed to the excellent corrosion resistance, mechanical property and processability[1]. Until now, the related researches[2-4] of Incoloy825 alloy are mainly focused on welding property, wear resistance, microstructure, and so on. Very limited literatures have been reported on its corrosion resistance[5-7]. Tan[8] has investigated the intergranular corrosion behavior of aged alloy. The samples aged at different temperature and time has different degree of sensitization. Li[9] indicated that 825 alloy had a better anticorrosion resistance than 600 alloy, which was attributed to its higher chromium content.

In Southeast coast of China, SO_2 is produced due to the industrial pollution, and dissolved into the seawater lead to the formation of $NaHSO_3$[10]. The presence of HSO_3^- ion may affect the corrosion status of metal operated in marine environment. It is well known that metal served in spray splash zone[11-13] exhibits very severe corrosion, which is attributed to the engineering structure under the condition of wetting-drying alternation. When Incoloy825 alloy is located at the marine splash zone, the existence of $NaHSO_3$ may further affect the electrode reaction process and anti-corrosion resistance. However, at present, no literature has been reported the corrosion behavior of Incoloy825 alloy in simulated SO_2 polluted seawater. Thus, it is necessary to investigate the theme.

In this work, the effect of $NaHSO_3$ concentration on the corrosion behavior of incoloy825 alloy in simulated seawater solution is studied by electrochemical measurements and periodic wet/day cycle corrosion test.

2. EXPERIMENTAL

The material used in this paper is a commercial incoloy825 alloy tube. The chemical composition of the alloy is (wt.%): Ni 46.00, Cr 23.50, Cu 3.00, Ti 1.20, Mo 3.50, Mn 1.00, Si 0.50, P 0.02, C 0.03, S 0.01 and Fe balance. Fig.1 shows the microstructure of the alloy. The alloy consists of single-phase of austenite (Υ), with clear grain boundary. The alloy sample (10 mm $\times$10 mm $\times$ 3mm) was packaged in epoxy resin, leaving an exposed region of 1 cm^2 as the working area. And then the samples were orderly grinded to 2000 grit SiC abrasive paper, polished with diamond paste to 1 μm, rinsed with deionized water and alcohol, and finally dried. The simulated SO_2 polluted seawater was prepared by adding different concentrations of $NaHSO_3$ (0, 0.05M, 0.1M) to 3.5% NaCl solution. The test solution temperature was kept constant at 30°C.

The tests were performed using periodic wet/day cycle corrosion system. One period was 1h, in the wet step, the samples were immerged into the solution bath, keeping at 30°C for 12 min, and maintained at the same temperature for 48 min in oven during the dry process. The relative humidity (RH) was controlled at 90%, and the experimental time was 18 days. After testing, the specimens were taken out for weight-loss analysis and electrochemical measurement. The electrochemical test of the samples was performed via a classical three-electrode cell using the PARSTAT2273 electrochemical workstation system. The alloy sample was served as working electrode, a saturated calomel electrode (SCE) as reference electrode, and a platinum plate as counter electrode. The open circuit potential (OCP) of the samples was tested for 0.5 h. Then EIS measurement was conducted at OCP in a frequency range from 100 kHz to 10 mHz with the disturbance AC signal amplitude of 10 mV. The potentiodynamic polarization curve was measured at a scanning speed of 1 mV/s from -0.8 V (vs SCE) to 0.5 V (vs SCE).

Prior to testing, the specimen was cleaned, dried and weighed. After the periodic wet/day cycle corrosion test, the corrosion product deposited on the sample surface was removed thoroughly. Subsequently, the sample was washed, dried, and weighed, and then the corrosion rate of alloy sample tested in 3.5% NaCl solution containing different concentrations of $NaHSO_3$ was calculated according to the weight-loss. The corrosion morphology of alloy sample was observed via SEM.
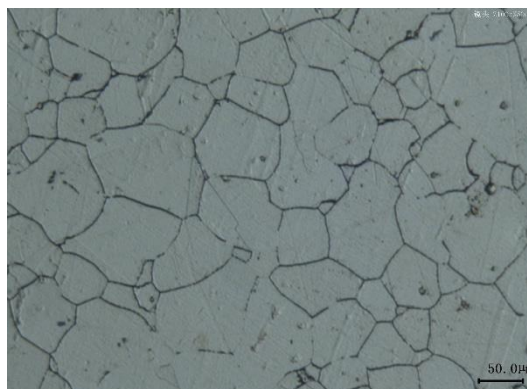
Figure 1. Microstructure of incoloy825 alloy

3. RESULTS

Figure 2 shows the open circuit potential of incoloy825 alloy tested in NaCl solution containing different concentrations of $NaHSO_3$. Firstly, the curves present the corrosion potential shifts negatively, and then moves positively as increasing $NaHSO_3$ concentration. That is, the corrosion potential of alloy tested at the absence of $NaHSO_3$ is the most positive, and the potential is the most negative while adding 0.05 M $NaHSO_3$. The more negative the potential value, the corrosion tendency the larger is. This indicates that the addition of $NaHSO_3$ could affect the corrosion tendency of alloy.
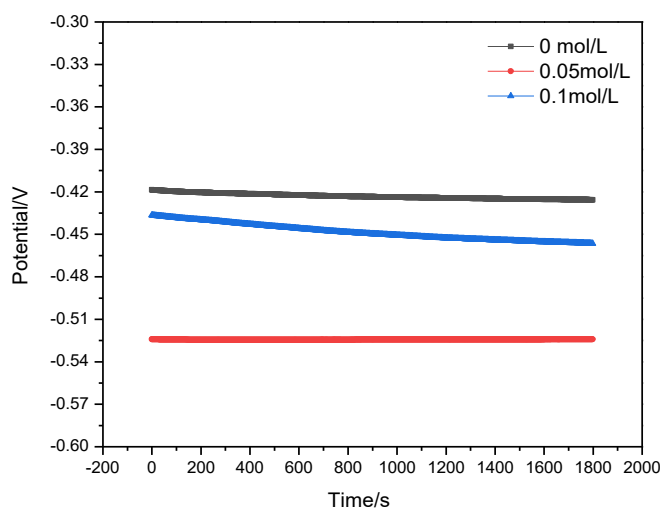

Figure 2. Open circuit potential of incoloy825 alloy in NaCl solution containing different concentrations of $NaHSO_3$
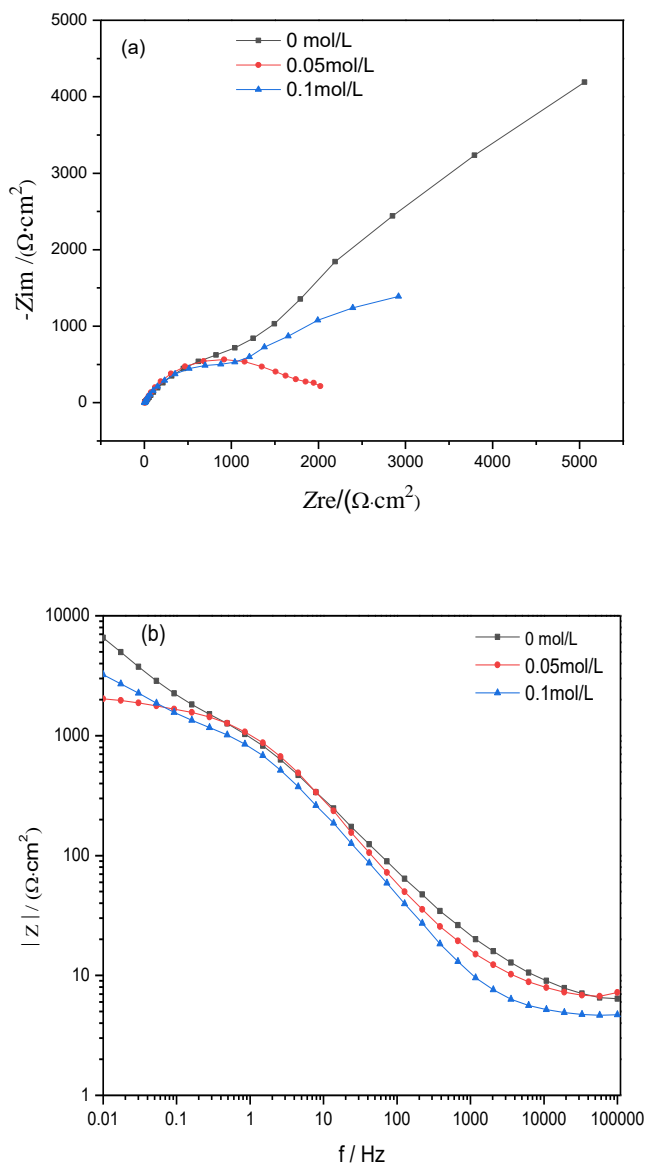
Figure 3. Impedance spectra of incoloy825 alloy measured in NaCl solution containing different concentrations of NaHSO$_3$ (a) Nyquist diagram, (b) Bode diagram.

Figure 3 shows the impedance spectra of incoloy825 alloy measured in NaCl solution containing different concentrations of NaHSO$_3$. As depicted in Fig.3a, the Nyquist curve presents the characteristics of capacitive arc, with different diameters of impedance semicircles in low frequency range. It is clearly found that the semicircle diameter of alloy reduces firstly and then increases with increasing NaHSO$_3$ concentration. The greater the diameter of capacitive arc, the better the corrosion resistance is [14]. This indicates that the addition of NaHSO$_3$ accelerates the corrosion of alloy. As shown in Bode plot (Fig.3b), without the addition of NaHSO$_3$, the alloy reveals the largest |Z| value, and the specimen tested in the solution with the addition of 0.05M NaHSO$_3$ has the lowest value in the low frequency. The larger the |Z| value, the greater the corrosion resistance is [15].

Using the equivalent circuit $R_s(Q_fR_f)(Q_{dl}R_{ct})$ to fit the impedance spectra. R_s is the solution resistance, and Q_f represents the capacitance of corrosion product film, coupled with the film resistance R_f. Q_{dl} represents the capacitance of double layer, and R_{ct} is the charge transfer resistance. As listed in Fig.4, as the increase of NaHSO$_3$ concentration, R_f and R_{ct} both decline firstly and then rise. The difference in R_f reflects that the corrosion product film formed on the alloy surface has different protective property. Among them, the film covered on the specimen tested without the addition of NaHSO$_3$ has a better protective property, compared with those with adding NaHSO$_3$. Similarly, R_{ct} value exhibits the same variation tendency. Without the presence of NaHSO$_3$, the largest R_{ct} value suggests the largest resistance to the charge transfer processes in the interface of metal/solution, i.e., the optimum corrosion resistance [16]. Thus, the addition of NaHSO$_3$ could decline the corrosion resistance of alloy.
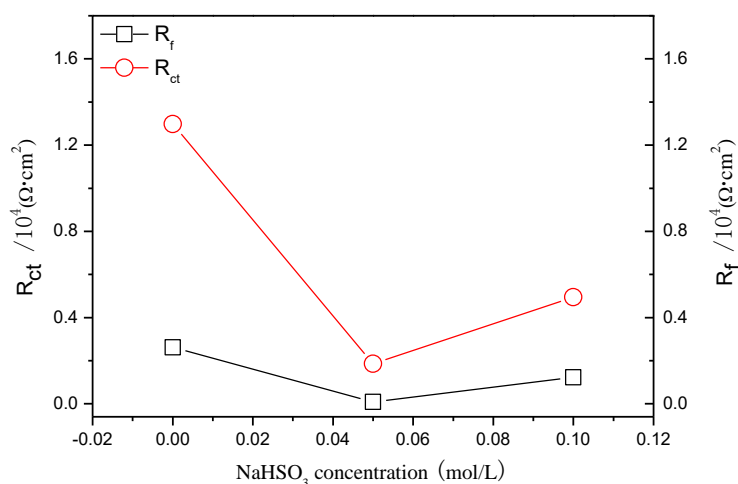

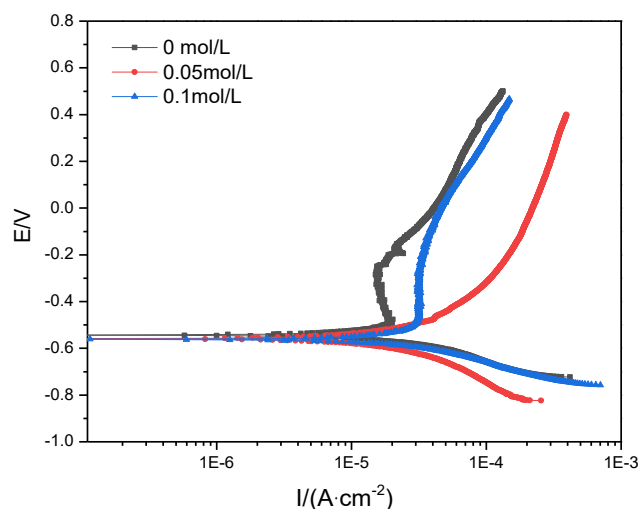**Figure 4.** The fitted R_f and R_{ct}

Figure 5. Polarization curve of alloy measured in NaCl solution containing different concentrations of NaHSO$_3$

Figure 5 presents the polarization curves of alloy samples measured in NaCl solution

containing different concentrations of NaHSO₃. The anode polarized curves display different characteristics. Without the addition of NaHSO₃ or at higher concentration of 0.1M NaHSO₃, the anode curves exhibit the similar passivation characteristic. Conversely, the obvious characteristic of activation dissolution is clearly observed in the curve when adding 0.05M NaHSO₃ to the solution. In this work, the curves are measured after corroding under periodic wet/dry cycle condition for 18d. And the corrosion product formed on the electrode surface may affect the corrosion status. At the absence of NaHSO₃, the corrosion product film has greater R_f value（Fig.4）, i.e., possesses better protective property. This may be due to its good compactness and integrity. Thus, the passivation characteristic is shown in the anode curve. On the contrary, under the condition of 0.05M NaHSO₃, the minimum R_f value suggests that the corrosion product may be nondense and broken, which can not prevent the corrosion effectively, resulting in the fast activation dissolution.

The fitted corrosion current densities are $15.63 \mu A \cdot cm^{-2}$, $40.40 \mu A \cdot cm^{-2}$ and $31.62 \mu A \cdot cm^{-2}$ respectively as the increasing NaHSO₃ concentration. Generally, the lower the corrosion current density value, the lower the corrosion rate is [17]. Consequently, the corrosion resistance reduces firstly and then increases with the increase of NaHSO₃ concentration. The result is in accord with the EIS test.
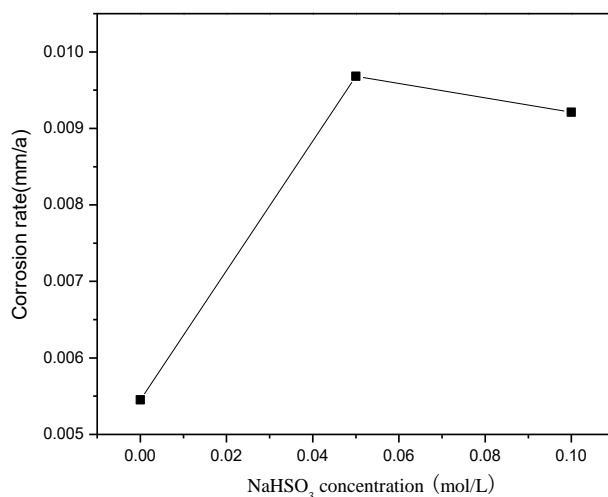

Figure 6. Corrosion rate of alloy measured in NaCl solution containing different concentrations of NaHSO₃

Fig.6 presents the corrosion rate of alloy measured in NaCl solution containing different concentrations of NaHSO₃. Obviously, the corrosion rate of the alloy increases firstly and then decreases with the increase of NaHSO₃ concentration, and the lowest value is exhibited without the addition of NaHSO₃. This means that the addition of NaHSO₃ promotes the corrosion, especially at 0.05M NaHSO₃.
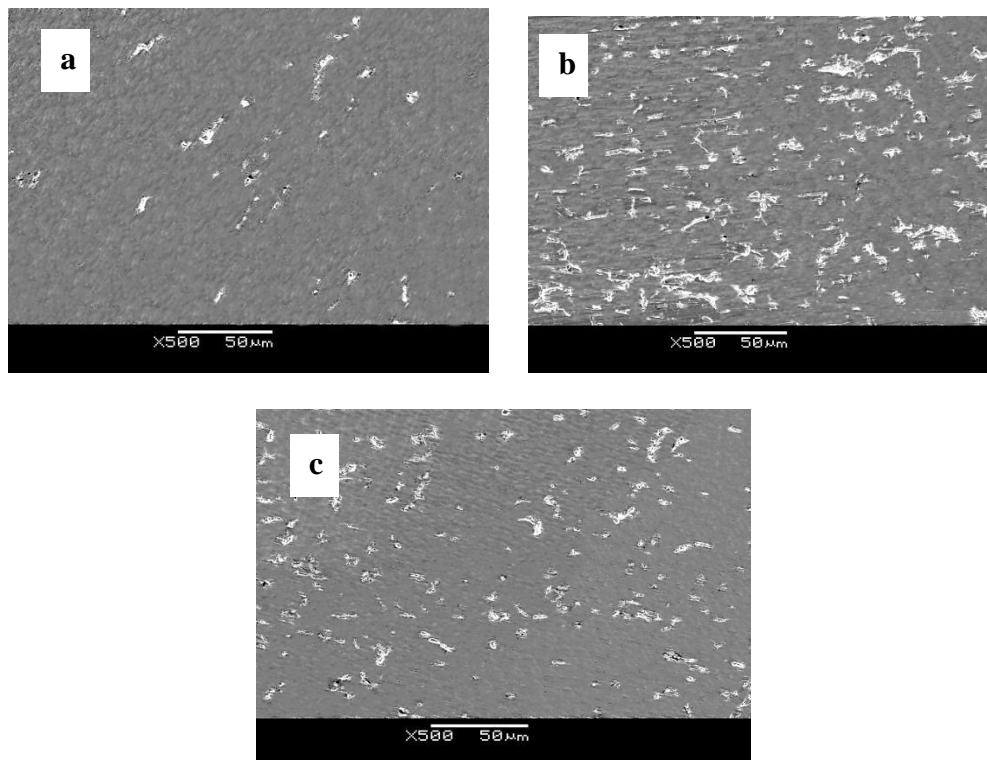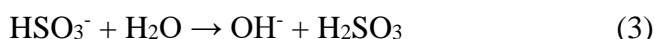
Figure 7. Surface corrosion morphology of alloy measured in NaCl solution containing different concentrations of NaHSO₃ after removal of corrosion products: (a) 0mol/L NaHSO₃; (b) 0.05mol/L NaHSO₃; (c) 0.1mol/L NaHSO₃

Fig. 7 reveals the surface corrosion morphology of alloy measured in NaCl solution containing different concentrations of NaHSO₃. There is an apparent difference in the corrosion status. As seen in Fig.7a, the corrosion degree is slight, with a few amount of small-sized pits sporadically distributed on the sample surface. And the most regions within surface area are hardly corroded. While adding NaHSO₃ to the solution, the corrosion becomes severe, with intensive pits formed on the specimen. This indicates that the addition of NaHSO₃ enhances the corrosion of alloy. Especially under the condition of 0.05mol/L NaHSO₃, the densest pits are distributed on the entire sample surface, and some small-sized pits dissolve together and form the large-sized one. This also demonstrates that the corrosion rate is the maximum at this condition, with the serious corrosion. As the further increase of NaHSO₃ concentration, the corrosion degree declines to some extent.

Known from the above all test results, the addition of NaHSO₃ accelerates the corrosion of alloy measured in NaCl solution, and the corrosion resistance reduces firstly and then increases with the augment of NaHSO₃ concentration. This may be attributed to the combined actions of two aspects, which are as follows: firstly, the addition of HSO_3^- could generate competitive adsorption on the alloy surface with Cl^- ion, decrease the adsorption of Cl^-, which causes the corrosion inhibition. On the other hand, the ionization action of HSO_3^- in the aqueous solution is stronger than hydrolysis reaction (shown in equations (1) (2) and (3)), which would generate the release of hydrogen ions and reduce the pH value of solution, resulting in the increase of corrosion degree. Thus, under the combined actions of the opposite effects, the addition of HSO_3^- firstly enhances the corrosion of alloy due to the acidification of solution, and then inhibits the corrosion because of competitive adsorption as the

further increase of NaHSO$_3$ concentration.

$$HSO_3^- \rightarrow H^+ + SO_3^{2-} \qquad\qquad (1)$$
$$O_2 + 2HSO_3^- + 2e \rightarrow 2H^+ + 2SO_4^{2-} \qquad\qquad (2)\ [18]$$
$$HSO_3^- + H_2O \rightarrow OH^- + H_2SO_3 \qquad\qquad (3)$$

4. CONCLUSIONS

The corrosion potential shifts negatively, and then moves positively with the increase of NaHSO$_3$ concentration. Meanwhile, the film resistance R$_f$ and charge transfer resistance R$_{ct}$ both decline firstly and then rise as the concentration change. And the anode polarization curves display different characteristics of passivation or activation. As the increasing addition of NaHSO$_3$, the corrosion rate of alloy increases firstly and then decreases. In the solution, the corrosion form of the alloy is mainly pitting corrosion, and the addition of NaHSO$_3$ increases the degree of pitting. The variation of the corrosion resistance as the increase of NaHSO$_3$ concentration may be attributed to the combined actions of solution acidification and competitive adsorption.

References

1. R. B. Rebak and P.Crook, *Adv. Mater. Process.,* 157(2000) 37.
2. N. Sayyar, M. Shamanian and B.Niroumand, *J. Mater. Process. Tech.,* 262(2018)562.
3. J. Kangazian and M. Shamanian, *J. Manuf. Process.,* 26(2017)407.
4. L.Yang, Z.Y.Geng, M.C. Zhang and J.X.Dong, *Proc. Eng.,* 27(2012)997.
5. S. A.Al-Fozan and A. U.Malik, *Desalination*, 228(2008)61.
6. Z.F.Yin, W.Z.Zhao, W.Y.Lai and X.H.Zhao, *Corros. Sci.,* 51(2009)1702.
7. T.Bellezze,G.Roventi and R.Fratesi, *Electrochim. Acta,* 49(2004)3005.
8. H. Tan, Y. M. Jiang, B. Deng, W.J.Gao and J.Li, *Nucl. Eng. Des.,* 241(2011)1421.
9. Y.H.Li, S.Z.Wang, X.Y.Tang, D.H.Xu, Y.Guo, J.Zhang and L.L.Qian, *Oxid. Met.,* 84(2015)509.
10. B. Deng, Y.M. Jiang, J. Gong, C.Zhong, J.Gao and J.Li, *Electrochim. Acta,* 53(2008)5220.
11. H. Meng, X. Hu and A. Neville, *Wear,* 263(2007)355.
12. K. M. Anwar Hossain, S. M. Easa and M. Lachemi, *Build. Environ.,* 44(2009)713.
13. S. Rivero, B. Chico and D. De la Fuente, *Rev. Metal. Madrid,* 43(2007)370.
14. C.R.Xue, L.H.Dong, T.Liu, F.Zhang, B.Yin and Y.S.Yin, *Corros. Sci. Prot. Technol.,* 24(2012)37.
15. F. Zhang, S.Chen, L.Dong, Y.Lei, T.Liu and Y.Yin, *Appl. Surf. Sci.,* 257(2011)2587.
16. X. Li, F. Xie, D. Wang, C.H. Xu, M. Wu, D.X. Sun and J.J. Qi, *Eng. Fail. Anal.,* 91(2018)275.
17. L.Freire, M.J.Carmezima and M.G.S.Ferreira, *Electrochim.Acta,* 56(2011)5280.
18. Q.T.Jiang, M.L.Ma, K.Zhang, X.G.Li, Y.J.Li, G.L.Shi, and J.W.Yuan, *J.Rare.Earth.,*32(2014)1170.